Biochimica et Biophysica Acta 939 (1988) 315–326
Elsevier

BBA 73924

Conformation of the polar headgroup of sphingomyelin and its analogues

K.S. Bruzik

Centre of Molecular and Macromolecular Studies, Polish Academy of Sciences, Lódź (Poland)

(Received 22 June 1987)
(Revised manuscript received 30 September 1987)

Key words: Sphingomyelin; Headgroup conformation; Phospholipid bilayer

The conformation of the polar headgroup of synthetic D-*erythro*-stearoylsphingomyelin (1), its L-*threo*-isomer (2) and phosphorothioyl analogues of 1 (3 and 4) has been studied in detail by high-resolution NMR spectroscopy. In both monomeric and aggregated states the phosphocholine function of 1 adopts the synclinal conformation (α_5 torsional angle), in analogy with phosphatidylcholine (Hauser, H., Guyer, W., Pascher, I., Skrabal, P. and Sundell, S. (1980) Biochemistry 19, 366–373). The conformation about the C1–C2 bond (θ_1 angle) of the sphingosine backbone is predominantly −synclinal, analogously to the conformation of the crystalline galactosyl cerebroside (Pascher, I. and Sundell, S. (1977) Chem. Phys. Lipids 20, 175–191). In contrast, the L-*threo*-isomer displays unrestricted rotation about C1–C2 bond. The possibility of the existence of a hydrogen bond between the 3-hydroxyl function and the bridged oxygen atom of sphingosine responsible for the different conformation of 1 and 2 is discussed. The modification of the phosphate function in 1 with sulfur has no significant effect on the conformation of the resulting analogues. The conformation of all studied compounds about the C–O phosphoester bonds (α_1 and α_4 torsion angles) is mainly antiperiplanar. Similar to other double-chain phospholipids, sphingomyelin shows a preference towards the antiperiplanar conformation about the C2–C3 bond.

Introduction

Despite the widespread occurrence of various sphingolipids in nature, the conformation of these lipids in monomeric and aggregated state is far less known compared to glycerol-based ones. Most of information regarding the structure and conformation of sphingolipids comes from the works of Abrahamsson [1,2] and Pascher [3,4] on lipid X-ray crystallography, and some related data are scattered amongst synthetic papers [5–8] or can be retrieved from the results on conformations of liposaccharides [9–12]. As was shown in the case of glycerophospholipids, the conformation in solution may be also a preferred one in the aggregated state [13,14]. The study presented in this paper is aimed at the elucidation of the conformation of sphingomyelin (2-*N*-acylsphingosyl-1-phosphocholine) in monomer state and of the effect of structural modification on its conformational properties.

As a basic structure we have chosen D-*erythro*-2-*N*-stearoylsphingosyl-1-phosphocholine (**1**), which is a representative sphingomyelin species

Abbreviations: SPsM, D-*erythro*-2-*N*-stearoylsphingosyl-1-thiophosphocholine, DMPC, 1,2-dimirystoyl-*sn*-glycero-3-phosphocholine; DLPE, 1,2-dilauroyl-*sn*-glycero-3-phosphoethanolamine; DMPA, 1,2-dimirystoyl-*sn*-glycero-3-phosphate; DPPsC, 1,2-dipalmitoyl-*sn*-glycero-3-thiophosphocholine; DMPG, 1,2-dimirystoyl-*sn*-glycero-3-phosphoglycerol.

Correspondence: K.S. Bruzik, Centre of Molecular and Macromolecular Studies, Polish Academy of Sciences, Boczna 5, 90-362 Lódź, Poland.

widely distributed in animals [15,16]. The analogues studied included L-*threo*-2-*N*-stearoylsphingosyl-1-phosphocholine (**2**) and (*S*p)- and (*R*p)-diastereomers of the phosphorothioyl analogue of **1**: (*S*p)-3 and (*R*p)-4 (see Scheme I). The ana-

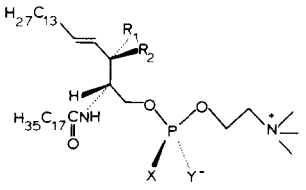

R_1 = H, R_2 = OH, X = Y = O ; D-erythro-SPM (1)
R_1 = OH, R_2 = H, X = Y = O, L-threo-SPM (2)
R_1 = H, R_2 = OH, X = O, Y = S; (S_p)-SP_5 M (3)
R_1 = H, R_2 = OH, X = S, Y = O; (R_p)-SP_5 M (4)

Scheme I. Structure of D-*erythro*-sphingomyelin and of its analogues studied.

logues were constructed to establish the role of the sphingosine 3-hydroxyl function and the phosphate function in determining conformation of sphingomyelin molecule. Our observations are frequently referenced to the phosphatidylcholine system, since the conformation of phosphatidylcholine is known in much greater detail [13,14,17–24]. It was also our intention to search for the link between the thermal phase behaviour of sphingomyelin bilayers [25] and conformational flexibility of this lipid. A recently performed calorimetric study of the phase behaviour of sphingomyelin analogues has pointed to the importance of the configuration at the carbon atom C-3 and at the phosphorus atom [25].

Methods

D-*erythro*-2-*N*-Stearoylsphingosyl-1-phosphocholine (**1**) and its analogues **2–4** used in this study were obtained and purified as described recently [6,25]. Cyclic 3′,5′-adenosine (*S*p)-phosphorothioate was from Boehringer. 1,2-Dipalmitoyl-*sn*-glycero-3-thiophosphocholine (**5**) was obtained as described [26]. ^{1}H, ^{13}C- and ^{31}P-NMR spectra were recorded on Bruker AM-500 and Bruker MSL-300 spectrometers. The spectra were acquired at 293 K unless otherwise stated. The experimental proton–proton coupling constants and chemical shifts were obtained from ^{1}H-NMR spectra by iterative simulation using the PANIC version of the LAOCOON computer simulation program. The input parameters for the simulation were obtained from the first-order analysis of the spectra (where applicable) and from the homodecoupling experiments. The simulated spectra shown in Figs. 2 and 3 were obtained by using the parameters of the high resolution spectra and their gradual changes to obtain the best fit.

Results

The results presented below follow the notation of torsional angles introduced by Sundaralingam [27] (see Scheme II). The analysis of populations

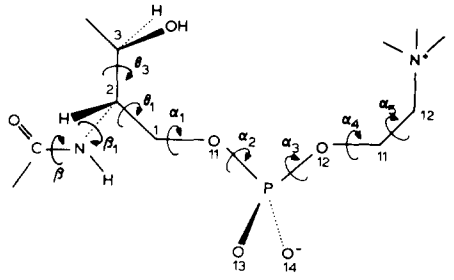

θ_3 ; C1-C2-C3-C4 α_3 ; O11-P-O12-C11
θ_1 ; O11-C1-C2-C3 α_4 ; P-O12-C11-C12
α_2 ; C2-C1-O11-P α_5 ; O12-C11-C12-N
α_2 ; C1-O11-P-O12

Scheme II. Notation of torsional angles of sphingomyelin headgroup according to Sundaralingam [27].

of staggered conformers is based on the Karplus relationship [28] between the magnitude of the three-bond coupling constant and the torsional angle as modified by Abraham and Gatti [29] and Haasnot et al. [30]. The component coupling constants used were either calculated using formulae derived by Haasnot et al. [30] for substituted ethanes and the Huggins element electronegativity [31], or assumed from low-temperature studies of conformations of substituted morpholines [32–34]. In the case of phosphatidylcholines, this type of approach has proved to produce data consistent with the results of X-ray crystallography [13,14]. X-ray crystallography data also provide the basis for considering exclusively staggered conformations in lipids [14,35–37]. Therefore, only the populational analysis of staggered rotamers about

carbon–carbon and carbon–oxygen bonds of the phospholipids' headgroup is dealt with in this report. All the staggered conformers considered are drawn in Scheme III and the collection of the experimental coupling constants used for calculations is presented in Table I.

The linewidth of 0.5–1.0 Hz observed in 500 MHz ^{1}H-NMR spectra of sphingomyelins **1**–**4** in methanol-d_4 solution indicates that, within the range of lipid concentration 4–50 mM, these compounds exist in this solvent as monomers. The representative spectra of **1** and **2** in $C^2H_3O^2H$ at their concentrations 4 mM along with insets of simulated spectra of the sphingomyelin headgroup are shown in Fig. 1. Several features apparent from these spectra and those reported earlier [6] seem noteworthy.

With the exception of choline protons of L-

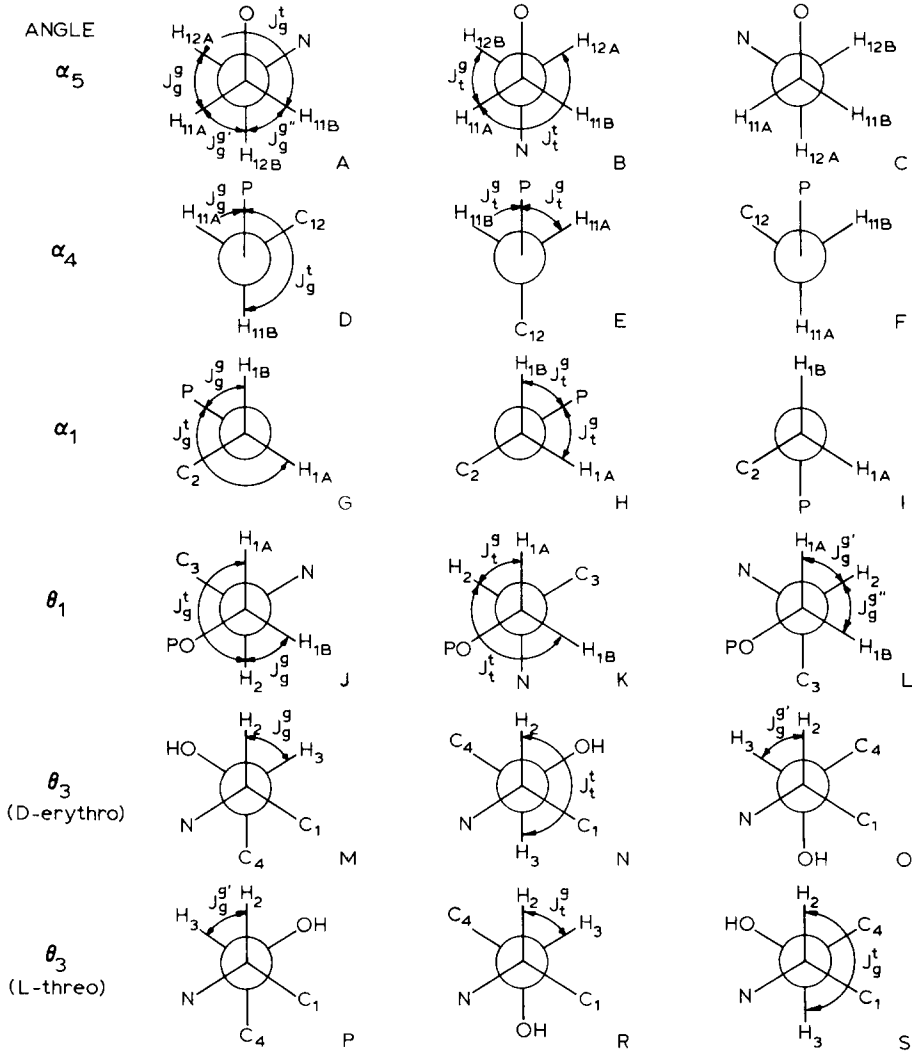

Scheme III. Minimum free energy conformations about carbon–carbon and carbon–oxygen bonds of the polar headgroup of sphingomyelin (See Scheme II for definitions of of torsional angles). The component vicinal couplings shown are as follows: θ_1 (calculated, Ref. 30): $J_t^g = 4.5$ Hz, $J_t^t = 10.8$ Hz, $J_g^t = 10.8$ Hz, $J_g^g = 3.9$ Hz, $J_g^{g'} = 2.2$ Hz, $J_g^{g''} = 1.6$ Hz; θ_3 (D-*erythro*, calculated, Ref. 30): $J_g^g = 3.0$ Hz, $J_t^t = 9.6$ Hz, $J_g^{g'} = 1.8$ Hz; θ_3 (L-*threo*, calculated, Ref. 30): $J_t^g = 1.3$ Hz, $J_t^g = 9.6$ Hz, $J_g^{g'} = 3.6$ Hz; α_1, α_4 (calculated, Ref. 20): $J_g^t = J_g^g = 1.77$ Hz, $J_g^t = 20.9$ Hz (Ref. 41): $J_g^t = J_g^g = 2.1$ Hz, $J_g^t = 23.0$ Hz; α_5 (calculated, Ref. 30, values in parentheses are experimental values from Ref. 39): $J_t^g = 4.29$ (5.48) Hz, $J_t^t = 11.93$ Hz (12.31) Hz, $J_g^g = 4.21$ Hz, $J_g^{g'} = 1.68$ Hz, $J_g^{g''} = 1.68$ Hz; $J_g^t = 11.93$ Hz, ($J_g^g + J_g^{g''} = 4.84$ Hz, $J_g^t + J_g^{g'} = 13.62$ Hz).

TABLE I

^{1}H-NMR COUPLING CONSTANTS OF PROTONS OF THE POLAR HEADGROUP OF SPHINGOMYELINS

All couplings were calculated from the 500 MHz ^{1}H-NMR spectra shown in Figs. 2 and 3; (**1**) $^3J_{POCC}$ values for C-2: 7.3 Hz, C_{12}: 8.0 Hz; (**2**) C-2: 8.0 Hz, C_{12}: 7.1 Hz; (**3**) C-2: 7.5 Hz, C_{12}: 8.3 Hz; (**4**) C-2: 7.7 Hz, C_{12}: 8.1 Hz; subscript A denotes one of the methylene protons resonating at lower field.

Coupling constant	D-*erythro*-**1**		L-*threo*-**2**		(*R*p)-**4** in $C^2H_3O^2H$	(*S*p)-**3** in $C^2H_3O^2H$
	in $C^2H_3O^2H$	in C^2HCl_3	in $C^2H_3O^2H$	in C^2HCl_3		
$^3J_{POH11A}$	6.90	6.90	6.79	7.5	8.23	8.23
$^3J_{POH11B}$	6.90	6.90	6.79	7.5	7.01	7.03
$^3J_{H11AH12B}$	7.08	7.08	7.02	7.1	2.27	2.27
$^3J_{H11BH12B}$				2.5	6.80	6.80
$^3J_{H11BH12A}$	2.46	2.46	2.49	7.0	2.18	2.18
$^3J_{H11AH12A}$				2.45	7.26	7.26
$^3J_{POH1A}$	6.53	7.2	6.40	7.0	8.09	7.80
$^3J_{POH1B}$	5.77	7.5	6.45	6.5	7.3	6.6
$^3J_{H1AH2}$	4.61	4.0	6.63	7.5	4.46	4.93
$^3J_{H1BH2}$	3.17	3.7	6.57	7.5	3.22	3.20
$^3J_{H2H3}$	8.0	7.0	3.19	3.1	8.15	7.95
$^3J_{H3H4}$	7.97		6.27		7.60	7.55
$^4J_{H3H5}$	0.5		1.30		0.5	0.7
$^4J_{POCCH_2}$	1.2		0.0		1.2	1.0

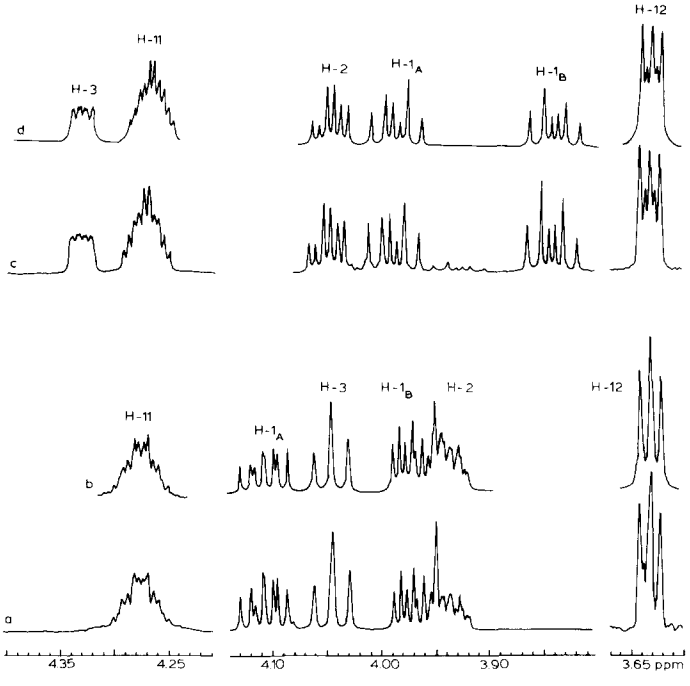

Fig. 1. Partial 500 MHz ^{1}H-NMR spectra of sphingomyelins in $C^2H_3O^2H$ at 4 mM concentration at the temperature 293 K; (a) D-*erythro*-sphingomyelin (**1**), (c) L-*threo*-sphingomyelin (**2**), (b, d) simulated spectra.

threo-**2**, most of geminal methylene protons in the spectra of sphingomyelins are both chemically and magnetically inequivalent. In the case of the 1-CH_2 protons of the sphingosine, the difference in the chemical shift is greater than 0.1 ppm. The geminal protons of the α-chain forming the MM'XX' spin system in the choline group of **1** are also inequivalent. This is contrasted with the analogous group of protons of **2** and phosphatidylcholine [13], where no shift difference is observed. The small differences in chemical shifts of geminal protons H-11A, H-11B and H-12A, H-12B in **1** are exclusively responsible for the different shape of its choline signals as compared to **2** (Fig. 1a, b), since no difference in pertinent coupling constants between **1** and **2** was observed (Table I).

The nonequivalence of choline protons H-11 is increased in the aggregated state of reversed micelles in C^2HCl_3, where two broad multiplets, at 4.28 and 4.35 ppm in **1** and at 4.29 and 4.35 in **2**, are observed (Fig. 2, concentration of **1** and **2**–**5** mM, traces a, c). At lower field (300 MHz) at the same temperature, the inequivalence of these protons is largely nullified (trace d). Interestingly, incorporation of sphingomyelin into reverse micelles has much smaller effect upon the chemical shifts of other protons (Table II). The chemical shift of the methine proton H-3 in **1** is not affected, but is shifted downfield by 0.11 ppm in **2**. Proton H-1A in **1** is displaced downfield by 0.063 ppm, but it is shifted upfield by 0.09 ppm in

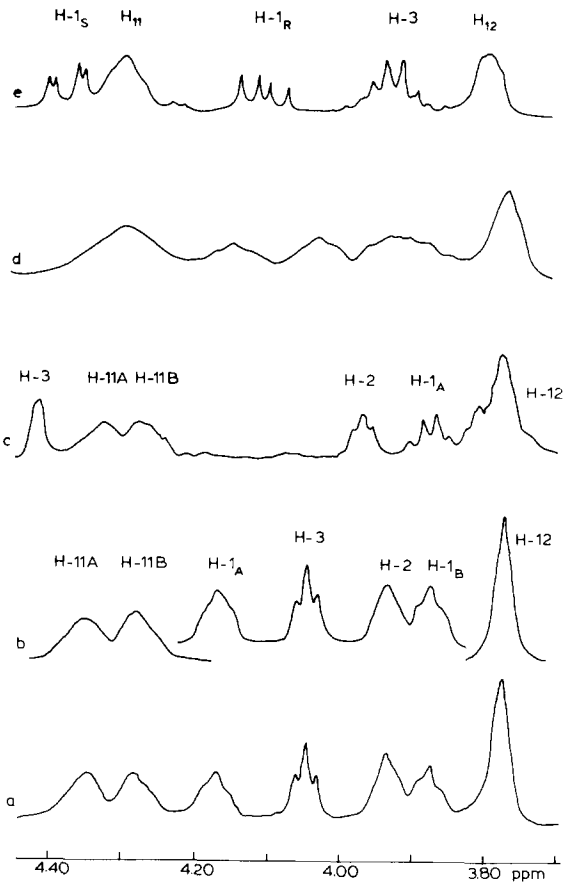

Fig. 2. Partial 500 MHz ^{1}H-NMR spectra of sphingomyelins in C^2HCl_3 at 5 mM concentration at the temperature 293 K; (a) D-*erythro*-sphingomyelin (**1**); (b) typical simulated spectrum, (c) L-*threo*-SPM (**2**); (d) 300 MHz spectrum of **1**; (e) 300 MHz spectrum of DPPC.

TABLE II

CHEMICAL SHIFTS OF PROTONS OF SPHINGOMYELIN POLAR HEADGROUPS AT 293 K

Proton position	D-*erythro*-sphingomyelin			L-*threo*-sphingomyelin			$\Delta\Delta\delta$ [b]
	in $C^2H_3O^2H$	in C^2HCl_3 [a]	$\Delta\delta$	in $C^2H_3O^2H$	in C^2HCl_3 [a]	$\Delta\delta$	
11_A	4.28	4.35	0.07	4.274	4.35	0.076	−0.006
11_B	4.26	4.28	0.02	4.274	4.29	0.016	−0.004
12_A	3.63	3.78	0.15	3.63	3.80	0.17	−0.02
12_B	3.63	3.78	0.15	3.63	3.80	0.17	−0.02
1_A	4.106	4.17	0.063	3.99	3.90	−0.09	0.153
1_B	3.97	3.87	−0.10	3.84	3.82	−0.02	−0.08
2	3.935	3.93	−0.005	4.05	3.99	−0.06	−0.055
3	4.05	4.05	0.0	4.33	4.44	0.11	−0.11
4	5.45	5.44	−0.01	5.45	5.40	−0.05	0.04
5	5.70	5.64	−0.06	5.73	5.70	−0.03	−0.03

[a] Simulated values.

[b] The difference of values in columns 3 and 6.

the case of **2**. The proton H-1B in both isomers is shifted upfield, but the change is far greater in **1** than in **2** (0.1 vs. 0.02 ppm, Table II). The vicinal coupling constants for choline group are alike in $C^2H_3O^2H$ and C^2HCl_3 for both isomers and these of sphingosine undergo rather insignificant alterations (Table I).

When compared to the behaviour of phosphatidylcholine, the aggregation of sphingomyelins in C^2HCl_3 causes much more line-broadening of the protons of the polar headgroup (Fig. 2e).

The increase in the difference of the chemical shift of H-11 protons is not observed on aggregation of D-*erythro*-sphingomyelin into normal micelles (in mixed solvent $C^2H_3O^2H/^2H_2O$). The simulation of the spectra shown in Fig. 3 (e.g., trace b vs. c) afforded the values of coupling constants accurate to within $\pm$ 0.5 Hz. Only small changes in the coupling constants and in the chemical shifts (simulated values) associated with aggregation were found in the latter solvent. Among the most affected were the choline protons, while H-3 and H-1 protons were not affected at all.

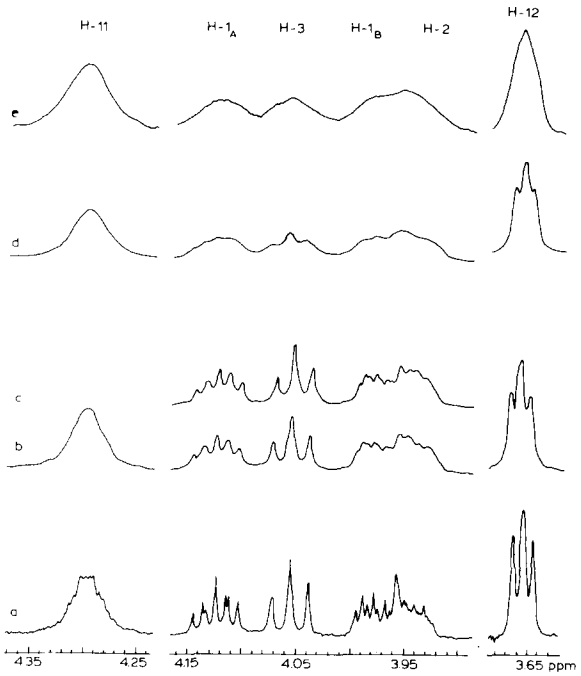

Fig. 3. 500 MHz ^{1}H-NMR spectra of D-*erythro*-sphingomyelin in $C^2H_3O^2H$ with increasing amounts of ^2H_2O; (a) 6.8%; (b) 10.9%; (c) simulation of spectrum b; (d) 12.3%; (e) 13.8% (v/v). Other conditions analogous to those in Fig. 1.

Methine proton H-3 displays a different chemical shift, depending on the configuration at C-3 of the sphingosine backbone, with H-3 in **2** shifted downfield by 0.28 ppm (4.05 in **1** and 4.33 in **2**). This situation is not mediated by sphingomyelin aggregation. Interestingly, a large difference in the chemical shifts of protons located at the glycerol 1-*sn* position (corresponding to position 3 in the notation adopted in this paper) is the common feature of all double-chain glycerophospholipids [13,17,23] and diacylglycerol. The proton shifted downfield (as in **2**) is usually coupled to H-2 with low coupling constant (approx. 3 Hz), whereas the upfield proton (as in **1**) has a coupling constant in the range 7–8 Hz. The removal of one of the fatty acid chains removes or strongly diminishes the chemical inequivalence of H-3 protons and the difference in their couplings to H-2 [21,22]. In the case of sphingolipids such as *erythro*-dihydrosphingosine and *threo*-dihydrosphingosine, $^3J_{H2H3}$ equals correspondingly 5.5 and 4.9 Hz. The scission of the P–O bond removes the difference in the chemical shifts of H-1 protons in both the sphingo- and glycerolipid series [6]. The removal of an α-chain abolishes the inequivalence of the methylene protons at C-1 (δ_{CH_2} 3.69 ppm, $^3J = 5.1$ Hz) in *N*-stearoylsphingosine and in unesterified hydroxymethylene function (δ_{CH_2} 3.66 ppm, $^3J =$ 5.4 Hz) of dipalmitoylglycerol in the spectra taken in methanol solution. In C^2HCl_3, most probably due to the formation of a new hydrogen bond of 1-OH to carbonyl group, the large downfield shift of H-3 (by 0.3 ppm) and the upfield shift of C-4 (by 2.1 ppm), and also a change in the respective coupling constants: $^3J_{H1AH2}$, 3.8 Hz; $^3J_{H1BH2}$, 3.1 Hz; $^3J_{H2H3}$, 3.2 Hz; $^3J_{H3H4}$ 6.3 Hz, are observed (see also Ref. 8).

The modification of phosphate with sulfur in **3** and **4** has virtually no influence on the chemical shifts of H-3 and H-2 protons, but it causes a downfield shift of protons vicinal to phosphorus, induces inequivalence of the H-11 and H-12 protons, and increases vicinal proton–phosphorus coupling constants [6].

The chemical shifts of amide protons in **1** and **2** (in C^2HCl_3) are highly sensitive to the temperature change ($5.8 \cdot 10^{-3}$ ppm/C° for **1** and $7.0 \cdot 10^{-3}$ ppm/C° for **2**). The corresponding vicinal coupling constants, $^3J_{HCNH}$, are 8.2 Hz and 6.7

TABLE III

ROTAMER POPULATIONS OF THE POLAR PART OF SPHINGOMYELINS IN METHANOL-d_4 AT 293 K

Bond	Torsional angle	Conformation	Population [a]	
			1	2
PO-CH_2CH [b,c]	α_1	antiperiplanar	0.61 (0.64)	0.58 (0.74)
		−synclinal	0.21	0.21
		+synclinal	0.18	0.21
PO-CH_2CH [c]	α_4	antiperiplanar	0.54 (0.74)	0.56 (0.62)
		−synclinal	0.23	0.22
		+synclinal	0.23	0.22
OCH_2-CH_2N [d,e]	α_5	±synclinal	1.00	1.00
		antiperiplanar	0.00	0.00
C1-C2 [d,f]	θ_1	+synclinal	0.26 (0.05)	0.16 (0.16)
		antiperiplanar	0.09 (0.31)	0.40 (0.42)
		−synclinal	0.65 (0.64)	0.44 (0.42)
C2-C3 [d,g]	θ_3	+synclinal	0.24 (0.45)	0.82 (0.47)
		antiperiplanar	0.76 (0.55)	0.18 (0.53)

[a] In mole fractions.

[b] Calculated using data from Ref. 40.

[c] Values in parentheses were obtained from $^3J_{POCC}$ using component coupling constants taken from Ref. 40; estimated error resulting from low digital resolution in ^{13}C-NMR spectra ±10%.

[d] Component coupling constants were calculated according to Ref. 30 (see caption to Scheme III).

[e] Using component coupling constants from the Ref. 39, the same rotamer populations were found.

[f] Values in parentheses are rotamer populations obtained via different assignment of diastereotopic protons H1A and H1B.

[g] Values in parentheses were calculated using component coupling constants given in Ref. 39.

Hz, respectively. These protons are also instantaneously exchanged by treatment with $C^2H_3O^2H$.

Populational analysis of staggered conformers

Molar fractions of staggered conformers of sphingomyelins with different torsional angles were calculated based on the component coupling constants taken from Partington et al. [38] (α_5) from Schleich et al. [39], Lee and Sarma [40] (α_1, α_4) or using the seven-parameter equation derived by Haasnot et al. [30] (θ_1, θ_3). In some instances, the vicinal coupling constants were adopted from the literature data obtained for the models structurally close to the system investigated. The fractional populations of staggered rotamers A–S shown in Scheme III are given in Table III.

Discussion

The conformation of the sphingomyelin headgroup is determined similarly to other phospholipids by the torsional angles α_1–α_6, β_1–β_3 and θ_1–θ_3 (Scheme II). The analysis of vicinal coupling constants obtained in this work does not afford information about the α_2, α_3 and β angles. Some indirect evidence comes from ^{31}P- and ^{13}C-NMR results [41–43]. The missing information could potentially be gathered by obtaining high-resolution proton-coupled ^{13}C-NMR spectra. With the sphingomyelin samples it was difficult to obtain sufficient resolution in ^{13}C-NMR as to obtain the desired long-range ^{1}H–^{13}C coupling constants. The scope of the present study had thus to be confined largely to the information arising from vicinal proton–proton, phosphorus–proton and phosphorus–carbon coupling constants.

The calculation of the time-averaged conformation of acyclic compounds is commonly based upon population analysis of staggered rotamers about a specific bond. For the purpose of these calculations, a knowledge of the component coupling constants is required. These values are normally obtained from the studies of model compounds with fixed geometry or can be calculated using the Karplus-type angular dependence of vicinal coupling constants. The Karplus equation

as modified by Haasnot et al. [30] was used to calculate vicinal proton–proton couplings. The use of this equation is advantageous because it accounts not only for the influence of the electronegativity of substituents attached to the carbon–carbon bond, but also for the spatial disposition of electronegative substituents with respect to coupled protons.

The values of $^3J_{HCOP}$ adopted were $^3J_t = 23$ Hz, $^3J_g = 2.1$ Hz from Lee and Sarma [40] and for $^3J_{CCOP}$, $^3J_t = 10$ Hz and $^3J_g = 2.5$ Hz from Schleich et al. [39]. The application of the equation given by Govil and Hosur [20] gives 20.9, 1.77 for $^3J_{HCOP}$ and 10.1, 2.07 Hz for $^3J_{CCOP}$, respectively. In the case of phosphorothioyl diester derivatives, no estimates of $^3J_{HCOP}$ could be found in the literature, therefore the respective values were obtained from ^{1}H-NMR spectra of the (*S*p)-isomer of cyclic 3′,5′-adenosine phosphorothioate. The corresponding values were $^3J_t = 23.4$ Hz and $^3J_g = 3.3$ Hz. These values are in agreement with the principle that for triester phosphorothioyl derivatives and a given POCH torsional angle (such as α_1 and α_4), the magnitude of the vicinal coupling constant, $^3J_{HCOP}$, usually exceeds the analogous value for phosphates [41,44].

α Angles

Inspection of the Table III shows that the choline group assumes the ± synclinal conformations A and C (Scheme III) about the C11–C12 bond. The result is analogous for all derivatives studied, regardless of whether the molar fractions of rotamers are deduced from *J* values reported earlier (e.g., from Partington et al. [38]) or calculated using the equation of Haasnot et al. [30] (see Table III). This result is in complete agreement with the conformations of various derivatives of choline in solution [13,17,21,22,38], in aggregated forms of phospholipids [13,21,22,45] and in crystals [36,37,46]. The invariance of choline conformation is suggestive of its control by the internal energetics of this functional group. It was postulated that nitrogen and oxygen atoms are kept in close proximity by electrostatic forces [17]. Since the corresponding H-11A, H-11B, and H-12A, H-12B protons in rotamers A and C are interchangeable by means of rotation about the C11–C12 bond, under the fast rotation condition their chemical shifts are averaged out, resulting in only small chemical shift difference such as the one observed for **1** in $C^2H_3O^2H$ (or equivalence such as in **2** or phosphatidylcholine). In a solvent of low dielectric constant like chloroform, both intra- and intermolecular ionic interactions strengthen and slow down the rate of rotation about this bond, resulting in the large chemical shift difference of the H-11 protons. If it is assumed that the effect which is exerted on the nearby proton by a positively charged nitrogen (H-11B in rotamer A and H-11A in C) is larger than that of the neutral oxygen atom, then a much smaller inequivalence of H-12 protons in the aggregated state is to be expected.

The conformation of sphingomyelin about C–O bonds (α_4 and α_1 angles) is predominantly antiperiplanar (E and H) with small amounts of ± synclinal conformers. The information from the three bond coupling constants is supplemented by additional evidence of the observation of the $^4J_{POCCH}$ between phosphorus and H-2 in **1**, **3** and **4** but not in **2**. Usually, a greater four-bond coupling constant is observed in the systems adopting the W-like conformation [41]. This situation parallels the one of other phospholipids [13] and acyclic nucleotides [40]. In the case of phosphorothioyl derivatives of phospholipids **3** and **4**, calculations of rotamer populations (based on $^3J_{POCH}$) indicate even stronger preference towards the antiperiplanar conformation. However, the magnitude of $^3J_{POCC}$ for carbons C-2 and C-12 of all studied sphingomyelins are equal within the experimental error, suggesting that no substantial conformational change about α_1 angle is taking place in sphingomyelin analogues **2**–**4** as compared to D-*erythro*-sphingomyelin. For all compounds of D-erythro series there is a slight preference towards one of the synclinal rotamers, as indicated by the inequality of $^3J_{POCH}$ for two H-1 protons (α_1). At the moment, it cannot be decided which of the synclinal rotamers, G or I, is the more abundant, since H-1 resonances were not assigned to pro-*R* or pro-*S* sites. The structural modifications in compounds **2**–**4** do not affect the average conformation about the α_4 angle.

θ Angles

θ_1 and θ_3 angles determine the disposition of

chains α, γ and β, γ, respectively, in relation to each other. In the case of natural D-*erythro*-sphingomyelin the most abundant conformer is $-$synclinal, L, with both H-1 methylene protons closely spaced with respect to the H-2 proton. The molar fractions of the conformers J and K are not known, since the H-1 protons have not been assigned their NMR signals. If it is assumed that the downfield proton, H-1A, is in its pro-*R* position (as actually shown in Scheme III, $^3J_{H1AH2} = 4.61$ Hz), then rotamers J and L are exclusive ones. If, on the other hand, proton H-1B is pro-*R*, then rotamer K accompanies L [50]. As a result, the molecule of D-*erythro*-sphingomyelin adopts a conformation analogous to the 'shovel' conformation found in the crystal structure of β-D-galactosyl-*N*-(2-D-hydroxyoctadecanoyl)-D-dihydroxysphingosine [1]. Sulfur substitution in the phosphate moiety exerts no effect and both isomers of SPsM are characterized by the same rotamer distribution about the C1–C2 bond, as in **1**. It is important to note that, in the absence of any stabilizing factors, rotamer L should not be the one of least energy, due to steric repulsions caused by the close proximity of the large atoms.

On the other hand, the L-*threo*-isomer, **2**, displays unrestricted rotation about the C1–C2 bond with all three staggered conformers J–L significantly populated. In this regard, the conformation of **2** resembles this of phosphatidylcholine in solution [13].

The precise analysis of the populations of rotamers about C2–C3 bond is limited by the fact that only one vicinal coupling constant is available. However, per analogy with the crystal structures of glycerophospholipids and cerebroside, the conformation O with substituents N and C-4 in the opposite arrangement has been neglected and two remaining, M and N, with these atoms in synclinal positions were considered in order to account for β- and γ-chain stacking. Employing calculated component coupling constants, the predominant antiperiplanar conformation, N, is predicted. The accuracy of the rotamer calculation in the case of the L-*threo*-isomer, **2**, suffers from a small difference in the calculated coupling constants for the two rotamers considered (1.3 and 3.6 Hz for R and P), with an estimated error of such calculation ± 0.5 Hz [30]. The application of these values suggests that rotamer P is the dominant one (Table III). The alternative use of the experimental coupling constants obtained in various model studies [32–34,47] also introduces uncertainties due to seemingly conflicting reports. The application of data from Refs. 32 and 47 leads to contradictory conclusions as to the participation of rotamers P and R. We propose the rotamer R is more abundant in this case, based on the following grounds: (i) relatively unrestricted rotation about C1-C2 bond in **2** (as opposed to **1**) requires that the 3-hydroxyl function be engaged in the interaction with a functionality other than phosphate or the bridged oxygen at C-1 (see the following section for the discussion of the H-bonding in sphingomyelin); (ii) the synclinal relation of amide nitrogen and 3-hydroxyl in R enables formation of an efficient H-bond between the carbonyl function and the hydroxyl group. (iii) The chemical shift of the H-3 proton in **2** is very close to this of H_{1S} while δ_H of H-3 in **1** is similar to pro-H_{1R} of phosphatidylcholine. Likewise, the coupling constants $^3J_{H2H3}$ in **1** (8.0 Hz) and in **2** (3.19 Hz) are analogous to the $^3J_{H2H1R}$ (7.0 Hz) and $^3J_{H2H1S}$ (3.3 Hz) of phosphatidylcholine [13,23]. In the latter case, based on the two coupling constants available, it was found that the rotamer with the chains γ and α in the antiperiplanar position is the dominant one [13,23]. This conformation is also found in the crystal structure of DMPC [36], DLPE [48], DMPA [37], DMPG [49] and cerebroside [1,3]. It is therefore reasonable to postulate that also in the case of **1** and **2** the analogous conformations N and R predominate, respectively. Although it is not possible at present to account for all factors controlling the chemical shift of the H-3 proton, it is clear that in the rotamer R the σ_{C-N} bond opposite to H-3 should create a substantial deshielding effect on this proton. Such an effect is absent in the rotamer N, where H-3 is antiplanar in relation to H-2.

Hydrogen bonding control of sphingomyelin headgroup conformation

The existence of stable hydrogen bonds stabilizing sphingolipid conformation in solids and in lipid bilayers has been postulated on several occasions [3,42,51]. The observation of the hindered rotation about the C1–C2 bond in D-*erythro*- but

not in L-*threo*-sphingomyelin suggests that in sphingomyelin the conformation about the θ_1 angle is particularly dependent on the configuration at C-3. As a possible explanation of this fact, we propose the formation of the hydrogen bond between the sphingosine hydroxyl function and the phosphoryl or the bridging oxygen stabilizing the +synclinal (J) and −synclinal (L) rotamers. In both rotamers, the oxygen atoms at the C-1 and C-3 carbon are in the synclinal positions (see also Fig. 5). The involvment of the amide function in the hydrogen bonding with the bridged oxygen is another explanation for the cause of the rotation restriction in case of **1**. The existence of such stabilization has been proposed in the case of the crystalline cerebroside [4]. The strong temperature dependence of the chemical shift of this proton in chloroform solution of D-*erythro*- and L-*threo*-sphingomyelin and their exchangeability disfavours this hypothesis in the case of sphingomyelin. The formation of the H-bond between the amide proton and phosphoryl oxygen can be also ruled out based on similar grounds and because it would require significant population of the synclinal conformation about O11–C1 bond.

We expect that a hypothetical hydrogen bond between the phosphate and the 3-OH function should vary the relative populations of rotamers about θ_1 in **1** and **2** and also about α_2 in **3** and **4**. Formation of such bond would require a population of *sc* rotamer about α_1 (equivalent to time-averaged torsional angle, α_1, significantly less than 180°) and a slight bend in θ_1. In view of the known dependence of the chemical shift of phosphorothioate diesters upon the protonation, phosphorothioyl analogues **3** and **4** should be particularly useful in the detection of the H-bond to the phosphate group. In (*R*p)-SPsM, the phosphoryl oxygen atom is in a suitable position for hydrogen bonding in the *sc* conformation (α_2) of the phosphate, while in the (*S*p)-isomer, formation of this bond would require a conformational change of the phosphate into an *ap* arrangement. If a hydrogen bond existed in both diastereomers, this would

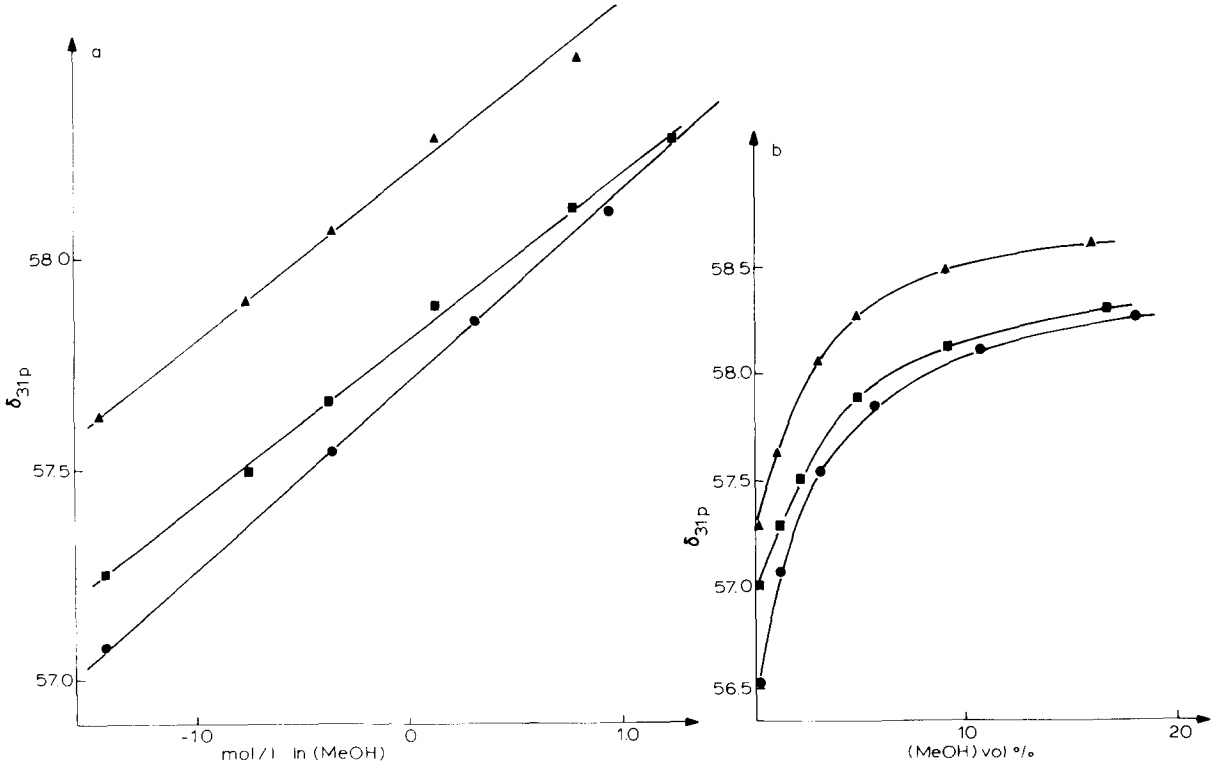

Fig. 4. Solvent dependence of the ^{31}P chemical shifts of thiosphingomyelins. Samples dissolved in C^2HCl_3 (5 mM) at 293 K were titrated with methanol. ■, (*S*p)-SPsM (**3**); ▲, (*R*p)-SPsM (**4**); ●, (*R*p)+(*S*p)-DPPsC.

result in a higher upfield shift in the ^{31}P-NMR of the (*R*p)-isomer than of the (*S*p) one in the solvent-enhancing H-bonds. In fact, the opposite is observed (Fig. 4). On the other hand, the formation of the intermolecular hydrogen bond to phosphate (e.g., with protic solvent after its addition) should lift or minimize the difference of the ^{31}P chemical shifts. In addition to the already reported NMR data [6], we have carried out the measurements of the chemical shifts of SPsM diastereomers in C^2HCl_3 titrated with methanol. As the reference compound in which no intramolecular hydrogen bonding to phosphodiester group occurs, the mixture of diastereomers of 1,2-dipalmitoyl-*sn*-glycero-3-thiophosphocholine, **5** (DPPsC) was chosen. The plot of these shifts as a function of methanol content is shown in Fig. 4. The largest chemical shift change takes place in the low range of methanol concentration, proving that the observed effect is due to the solvation of the phosphorothioyl function rather than caused by change in the medium polarity. It is clear that the solvent dependence of the chemical shift is steeper in the case of (*R*p)-SPsM than in (*S*p)-SPsM. DPPsC displays the highest sensitivity to methanol additions but, nonetheless, overall differences between the behaviour of (*R*p)-SPsM, (*S*p)-SPsM and DPPsC are small. The behaviour of D-*erythro*-sphingomyelin is very similar to L-*threo*-sphingomyelin (data not shown). As the rotamer populations about θ_1 are very close in all *erythro* compounds, the stabilization of $-sc$ conformation takes place regardless of sulfur substitution. We conclude therefore, that the acceptor site of the hypothetical hydrogen bonding in D-*erythro*-sphingomyelin is the bridging ester oxygen atom rather then the phosphoryl oxygen. The formation of the hydrogen bonding would be possible in the motion-averaged conformation represented in Fig. 5.

In the case of L-*threo*-sphingomyelin, the formation of this hydrogen bond could be prevented by the engagement of the 3-hydroxyl function in another hydrogen bond, e.g., with the carbonyl function. In fact, the predominant rotamer about the θ_3 angle is R (see above discussion on θ_3 angle in **2**) with the nitrogen atom in the vicinity of the hydroxyl function. However, the existence of such hydrogen bond in **2** would require a β_1 angle of

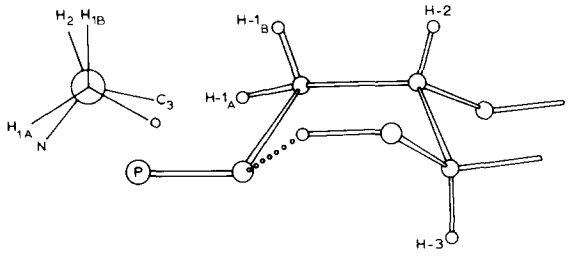

Fig. 5. The most probable, motion-averaged conformation of the sphingosine backbone region of D-*erythro*-sphingomyelin.

approx. $-120°$ instead of the $120°$ normally found in most lipids [4,14], and no clear-cut evidence for this hydrogen bond is available at this time.

The conformational study presented in this paper lends some support to the hypothesis that recently observed differences in the thermal phase behaviour of **1** and **2** may be caused by the different molecular conformation of these compounds [25]. Although the different phases undergoing transitions were not characterized, it was observed that the behaviour of **2** is analogous to that of saturated phosphatidylcholines, while synthetic **1** displays complicated metastable behaviour. The major differences in phase behaviour were also observed in hydroxy-fatty acids containing cerebroside and palmitoyl cerebroside [52]. It is not possible at present to provide decisive evidence for the control of these phenomena by the conformational properties of molecules. Further study to solve this problem is in progress.

Acknowledgments

The author is very grateful to Dr. Ming-Daw Tsai of The Chemistry Department, The Ohio State University, Columbus, OH for generous support. This work was supported in part by a research grant from the National Institute of Health to Dr. Ming-Daw Tsai (No. GM 30327), and from the Polish Academy of Sciences (No. CPBP 01.13.3.16). The 500 MHz ^{1}H-NMR spectra were obtained at the Campus Instrumentation Center of The Ohio State University and were supported by grant RR 01458 (to M.-D.T).

References

1 Abrahamsson, S., Dahlen, B., Lofgren, H., Pascher, I. and Sundell, S. (1977) in Structure of Biological Membranes, 34th Nobel Symp. Skovde, Sweden 1976 (Abrahamsson S. and Pascher I., eds.), pp. 1–23, Plenum Press, New York.

2 Karlsson, K.-A. (1977) in Structure of Biological Membranes, 34th Nobel Symp., Skovde, Sweden 1976 (Abrahamsson S. and Pascher I., eds.), pp. 245–274, Plenum Press, New York.

3 Pascher, I. (1976) Biochim. Biophys. Acta 455, 433–451.

4 Pascher, I. and Sundell, S. (1977) Chem. Phys. Lipids 20, 175–191.

5 Cohen, R., Barenholz, Y., Gatt, S. and Dagan, A. (1984) Chem. Phys. Lipids 35, 371–384.

6 Bruzik, K.S. (1988) J. Chem. Soc., Perkin Trans., in press.

7 Tkaczuk, P. and Thornton, E.R. (1981) J. Org. Chem. 46, 4393–4398.

8 Julina, R., Herzig, T., Bernet, B. and Vasella, A. (1986) Helv. Chim. Acta 69, 368–373.

9 Dabrowski, J., Hanfland, P. and Egge, H. (1980) Biochemistry 19, 5622–5658.

10 Hanfland, P., Egge, H., Dabrowski, U., Kuhn, S., Roelcke, D. and Dabrowski, J. (1981) Biochemistry 20, 5310–5319.

11 Sarmientos, F., Schwarzmann, G. and Sandhoff, K. (1985) Eur. J. Biochem. 146, 59–64.

12 Shashkov, A.S., Smirnowa, G.P., Chekareva, N.V. and Dabrowski, J. (1986) Bioorg. Khim. 12, 789.

13 Hauser, H., Guyer, W., Pascher, I., Skrabal, P. and Sundell, S. (1980) Biochemistry 19, 366–373.

14 Hauser, H., Pascher, I., Pearson, R.H. and Sundell, S. (1981) Biochim. Biophys. Acta 650, 21–51.

15 Barenholz, Y. and Gatt, S. (1982) in Phospholipids, pp. 129–177, (Hawthorne J.N. and Ansell G.B., eds.), pp. 129–177, Elsevier, Amsterdam.

16 Barenholz, Y. and Thompson, T.E. (1980) Biochim. Biophys. Acta 604, 129–158.

17 Birdsall, N.J.M., Feeney, J., Lee, A.G., Levine, Y.K. and Metcalfe, J.C. (1972) J. Chem. Soc., Perkin Trans. 2, 1441–1445.

18 London, R.E. Walker, T.E., Wilson, D.M. and Matwiyoff, N.A. (1979) Chem. Phys. Lipids 25, 7–14.

19 Ramaswamy, M., Mohammed, M.A., Abd El-Rahman, M.M.A., Wedmid, Y., Parthasarathy, S. and Baumann, W.J. (1982) J. Org. Chem. 47, 2158–2163.

20 Govil, G. and Hosur, R.V. (1982) Conformation of Biological Molecules (Diehl P., Fluck E. and Kosfeld R., eds.), p. 155 Springer-Verlag, Berlin.

21 Hauser, H., Guyer, W., Levine, B., Skrabal, P. and William, R.J.P. (1978) Biochim. Biophys. Acta 508, 450–463.

22 Hauser, H., Guyer, W., Spiess, M., Pascher, I. and Sundell, S. (1980) J. Mol. Biol. 137, 165–182.

23 Akutsu, H. and Kyogoku, Y. (1977) Chem. Phys. Lipids, 18, 285–303.

24 Fendler, J.H. (1982) in Biomembrane Mimetic Chemistry, p. 113–183 J. Wiley, New York.

25 Bruzik, K.S. and Tsai, M.-D. (1987) Biochemistry 26, 5364–5368.

26 Bruzik, K.S., Salamończyk, G. and Stec, W.J. (1986) J. Org. Chem. 51, 2368–2370.

27 Sundaralingam, M. (1972) Ann. N.Y. Acad. Sci. USA 195, 324–355.

28 Karplus, M. (1959) J. Chem. Phys. 30, 11.

29 Abraham, R.J. and Gatti, G. (1969) J. Chem. Soc. (B) 961–968.

30 Haasnot, C.A.G., De Leeuw, F.A.A.M. and Altona, C. (1980) Tetrahedron 36, 2783–2792.

31 Huggins, M.L. (1953) J. Am. Chem. Soc. 75, 4123–4126.

32 Hernestam, S. and Nilsson, B. (1976) Org. Magn. Res. 8, 582–586.

33 Brugel, W. (1969) Org. Magn. Res. 1, 425–430.

34 Spragg, R.A. (1968) J. Chem. Soc. (B), 1128.

35 Hauser, H., Pascher, I. and Sundell, S. (1980) J. Mol. Biol. 137, 249–264.

36 Pearson, R.H. and Pascher, I. (1979) Nature 281, 499–501.

37 Hitchcock, P.B., Mason, R., Thomas, K.M. and Shipley, G.G. (1974) Proc. Natl. Acad. Sci. USA 71, 3037–3040.

38 Partington, P., Feeney, J. and Burgen, A.S.V. (1972) Mol. Pharmacol. 8, 269–277.

39 Schleich, T., Cross, B.P. and Smith, I.C.P. (1976) Nucleic Acids Res. 3, 355–370.

40 Lee, C.-H. and Sarma, R.H. (1976) J. Am. Chem. Soc. 98, 3541–3548.

41 Gorenstein, D.G. (1984) in Phosphorus-^{31}P-NMR (Gorenstein D.G., ed.), pp. 7–36, Academic Press, New York.

42 Schmidt, C.F., Barenholz, Y. and Thompson, T.E. (1977) Biochemistry 16, 2649–2656.

43 Henderson, T.O., Glonek, T. and Meyers, T.C. (1973) Biochemistry 13, 623.

44 White, D.W. and Verkade, J.G. (1970) J. Magn. Res. 3, 111–116.

45 Seelig, J., Gally, H.-U. and Wohlgemuth, R. (1977) Biochim. Biophys. Acta 467, 109–119.

46 Abrahamsson, S. and Pascher, I. (1966) Acta Crystallogr. 21, 79–87.

47 Zefirov, N.S., Gurvich, L.G., Shashkov, A.S., Krimer, M.Z. and Vorobeva, E.A. (1976) Tetrahedron 32, 1211–1219.

48 Harlos, K., Eibl, H., Pascher, I. and Sundell, S. (1984) Chem. Phys. Lipids 34, 115–126.

49 Pascher, I., Sundell, S., Harlos, K. and Eibl, H. (1987) Biochim. Biophys. Acta 896, 77–88.

50 Meulendijkis, G.H.W.M., Van Es, W., De Haan, J.W. and Buck, H.M. (1986) Eur. J. Biochem. 157, 421–426.

51 Boggs, J.M. (1980) Can. J. Biochem. 58, 755–770.

52 Curatolo, W. (1982) Biochemistry 21, 1761–1764.